A&A 535, A27 (2011)
DOI: 10.1051/0004-6361/201117220

Astronomy & Astrophysics

When sticking influences H_2 formation

S. Cazaux[1], S. Morisset[2], M. Spaans[1], and A. Allouche[2]

[1] Kapteyn Astronomical Institute, PO box 800, 9700AV Groningen, The Netherlands
e-mail: cazaux@astro.rug.nl
[2] Laboratoire de Physique des Interactions Ioniques et Moléculaires, UMR CNRS 6633, Université de Provence, Campus de Saint-Jérôme, case 242, 13397 Marseille Cedex 20, France

Received 9 May 2011 / Accepted 29 August 2011

ABSTRACT

Aims. Because of their catalytic properties, interstellar dust grains are crucial to the formation of H_2, the most abundant molecule in the Universe. The formation of molecular hydrogen strongly depends on the ability of H atoms to stick on dust grains. In this study we determine the sticking coefficient of H atoms chemisorbed on graphitic surfaces, and estimate its impact on the formation of H_2.
Methods. The sticking probability of H atoms chemisorbed onto graphitic surfaces is obtained using a mixed classical-quantum dynamics method. In this, the H atom is treated quantum-mechanically and the vibrational modes of the surface are treated classically. The implications of sticking for the formation of H_2 are addressed by using kinetic Monte Carlo simulations that follow how atoms stick, move and associate with each other on dust surfaces of different temperature.
Results. In our model, molecular hydrogen forms very efficiently for dust temperatures lower than 15 K through the involvement of physisorbed H atoms. At dust temperatures higher than 15 K and gas temperatures lower than 2000 K, H_2 formation differs strongly if the H atoms coming from the gas phase have to cross a square barrier (usually considered in previous studies) or a barrier obtained by density functional theory (DFT) calculations to become chemisorbed. The product of the sticking times efficiency can be increased by many orders of magnitude when realistic barriers are considered. If graphite phonons are taken into account in the dynamics calculations, then H atoms stick better on the surface at high energies, but the overall H_2 formation efficiency is only slightly affected. Our results suggest that H_2 formation can proceed efficiently in photon-dominated regions, X-ray dominated regions, hot cores and in the early Universe when the first dust is available.

Key words. astrochemistry – ISM: abundances – ISM: molecules – molecular processes

1. Introduction

Interstellar dust grains play a very important role in the chemistry of the interstellar medium (ISM). Because of inefficient gas phase paths to form H_2, dust grains are considered as the favored habitat to form H_2 molecules (Gould & Salpeter 1963). In the past decades, a plethora of laboratory experiments and theoretical models have been developed to understand how the most abundant molecule of the Universe forms. The sticking of H atoms on surfaces has received considerable attention because this mechanism governs the formation of H_2, but also other molecules that contain H atoms. The sticking of H atoms on dust grains can also be an important mechanism to cool interstellar gas (Spaans & Silk 2000). As H atoms arrive on the dust, they can be weakly bound (physisorbed) or strongly bound (chemisorbed) to the surface. The sticking of H in physisorption state has been highlighted by several experiments on different type of surfaces (Pirronello et al. 1997b, 1999, 2000; Perry & Price 2003). Experiments performed on surfaces at higher temperatures revealed how H atoms stick in chemisorbed state (Zecho et al. 2002; Hornekær et al. 2006; Mennella 2006). In addition, theoretical studies confirmed that the sticking of H atoms varies strongly with gas and dust temperatures (Leitch-Devlin & Williams 1985; Buch 1989; Sha et al. 2005; Medina & Jackson 2008; Morisset & Allouche 2008; Cuppen et al. 2010; Morisset et al. 2010). To study the sticking of an atom on a surface, it is necessary to take into account the vibrational modes (phonons) of the surface (Burke & Hollenbach 1983; Buch 1989; Morisset & Allouche 2008; Morisset et al. 2010).

In the ISM, dust grains are mainly carbonaceous particles or silicates, with various sizes, and a large part of the available surface for chemistry is in the form of very small grains or polyaromatic hydrocarbons (PAHs; Weingartner & Draine 2001). These PAHs have similar characteristics as graphite surfaces, as shown by different calculations (Jeloaica & Sidis 1999; Sha & Jackson 2002; Ferro et al. 2008). Jeloaica & Sidis (1999) studied the interaction between H atoms and a coronene, whereas Ferro et al. (2008) and Sha & Jackson (2002) determined the H-graphite interaction. All these theoretical works obtained identical characteristics: the H atom coming from the gas phase can physisorb (43 meV) or chemisorb (0.76 eV) on the graphite or PAH. Several experimental studies showed that H atoms can physisorb on carbonaceous (Pirronello et al. 1997b; 1999; 2000), silicates (Pirronello et al. 1997a) and graphitic (Perry & Price 2003) surfaces, and can also chemisorb on graphite surfaces (Zecho et al. 2002; Hornekær et al. 2006). These experiments revealed that adsorption of H atoms (physisorption and chemisorption) is of key importance to form H_2 for a wide range of dust and gas temperatures, as observed in the ISM. The H atom can chemisorb only on top of a C atom and a surface reconstruction is observed: the C atom goes out of the surface plane. This phenomenon is called puckering and creates a barrier against chemisorption of 0.2 eV (Jeloaica & Sidis 1999; Sha & Jackson 2002; Ferro & Allouche 2003; Hornekær et al. 2006). This barrier is important and does not allow an efficient sticking mechanism for atoms coming in at low energies. Therefore, sticking through chemisorption strongly depends on the energy of the

incoming atoms. Also, the sticking is sensitive to the temperature of the dust because the surface excitation modes play a role in redistributing the excess energy of an atom.

The H_2 formation occurs through Eley-Rideal (ER) or Langmuir-Hinshelwood (LH) mechanisms. In the ER mechanism, an H atom coming from the gas phase collides with an H atom that is initially adsorbed (chemisorbed) on the graphite surface. Theoretical (Rougeau et al. 2006; Ferro et al. 2008) and experimental (Hornekær et al. 2006) studies show that H atoms are chemisorbed on the surface in dimer configurations (2 H atoms located in the same benzenic ring), and that two hydrogen dimers configurations are stable: the ortho-dimer and the para dimer (Fig. 3, bottom panel). Density functional theory (DFT) calculations show that while the chemisorption of one H atom is associated with an important barrier, the formation of the para dimer is barrier-less and that the formation of the ortho dimer has a reduced barrier (Rougeau et al. 2006). The formation of H_2 that involves chemisorbed atoms through the ER mechanism has been studied by DFT (Jeloaica & Sidis 1999; Sha & Jackson 2002; Ferro & Allouche 2003) and dynamics calculations (Rutigliano et al. 2001; Ree et al. 2002; Sha & Jackson 2002; Morisset et al. 2003; 2004b; Martinazzo & Tantardini 2006). Based on these calculations, different mechanisms have been proposed to contribute to the H_2 formation through the ER mechanisms: the direct ER that involves isolated H atoms (monomers, Sha & Jackson 2002; Morisset et al. 2003; 2004b; Martinazzo & Tantardini 2006), barrier-less formation of H_2 involving one H atom in a para-dimer configuration (Bachellerie et al. 2007) and formation by diffusing H atoms in physisorbed states (Bonfanti et al. 2007). In the LH mechanism, the two H atoms are adsorbed (physisorbed) on the graphite surface, diffuse on the surface and collide to desorb in a hydrogen molecule. This mechanism has also been studied (Morisset et al. 2004a; 2005; Martinazzo & Tantardini 2006). The different mechanisms to form H_2 on graphite surfaces are the following:

M1) LH mechanism: two physisorbed H atoms encounter each other on the surface;
M2) direct Eley-Rideal mechanism involving H atom chemisorbed in a monomer (only one H atom chemisorbed on the cycle, Fig. 3, bottom panel);
M3) direct Eley-Rideal mechanism involving an H atom chemisorbed in a dimer (H atom chemisorbed on a cycle where an H is already present: dimer position on the first cycle, Fig. 3, bottom panel);
M4) fast diffusion of physisorbed H atoms that enter chemisorbed sites occupied by H atoms (monomer);
M5) fast diffusion of physisorbed H atoms that enter chemisorbed sites occupied by H atoms (dimer);
M6) direct Eley-Rideal mechanism involving an H atom in meta, 5 and S (second cycle) positions (Dumont et al. 2008, see Fig. 3 bottom panel);
M7) ER mechanism by fast diffusing H atoms in the physisorption state (Bonfanti et al. 2007).

Recent experimental studies (Lemaire et al. 2010; Islam et al. 2007) show that the ro-vibrationnal states of the H_2molecule formed on the surface can be detected (silicates and graphite). The ro-vibrationnal distribution of the H_2 allows one to classify the LH and the ER mechanisms to form the molecule as function of the dust temperature. Experimentally, it is not possible to identify the M1 to M7 mechanisms proposed to form H_2. The objective of our work is to classify the predominant mechanisms to form H_2 as a function of gas and dust temperature. In each proposed mechanism, the sticking of the H atoms in physisorption sites and chemisorption sites (Fig. 3 top panel) is crucial to allow the H_2 formation. In this study we concentrate on understanding how the first H atom chemisorbs on the grain with a direct ER mechanism and how the sticking probability impacts the H_2 formation. During the collision between an atom and a surface, the collisional energy is distributed between the vibrational excitation of the newly formed bond and the vibrational modes of the surface.Therefore, to calculate the sticking of atoms on a surface in a realistic way, one has to consider the lattice dynamics. For this purpose, we study the interaction of H atoms with graphitic surfaces, which are surfaces with similar properties as PAH surfaces. Our attention focusses particularly on these surfaces because PAHs represent a large part of the total surface area of dust grains (up to 50%, Weingartner & Draine 2001).

In the first section, the time-dependent dynamics method is presented to study the sticking of H atoms in chemisorbed sites on the graphite surface in the collinear geometry. In the subsequent section, the different mechanisms for the formation of H_2 are implemented into the kinetic Monte Carlo (KMC) simulations. The sticking probability obtained by the dynamics method is included in the KMC code. In the last section we assess how this sticking changes the processes involved in the formation of H_2 and identify the predominant mechanisms to form H_2 molecules as function of the gas and dust temperature.

2. Sticking: dynamical calculations

In this section the time-dependent wave packets propagation method is presented to calculate the transmission probability for an H atom to overcome the chemisorption barrier. The time-dependent dynamics method, which takes into account vibrational modes of the surface, is used to calculate the sticking probability of H atoms in chemisorbed sites on a graphite surface. Our calculation are performed in the collinear approach.

2.1. The wave packet propagation method

This method solves for the time-dependent Schrödinger equation:

$$i\hbar \frac{\partial |\psi(t)\rangle}{\partial t} = H |\psi(t)\rangle , \quad (1)$$

where H is the Hamiltonian of the H-graphite system, which is the sum of a kinetic operator and a potential operator and $|\psi(t)\rangle$ is the time-dependent wave function. This method consists of choosing an initial wave function (at time $t = 0$) to model the H atom in the gas phase. The application of the evolution operator on the wave function allows us to obtain the wave function at time $t + \Delta t$. The time propagation is performed using a Lanczos method (Leforestier et al. 1991). The kinetic operator is applied on the wave function using a Fourier method (Kosloff & Kosloff 1983). The propagated wave function is analyzed by a flux analysis method (Balint Kurti et al. 1990) to obtain physical information such as the probability of transmission of a potential barrier.

2.2. The probability of transmission of the chemisorption barrier

The interaction potential between the H atom and the graphite surface is well known (Ferro & Allouche 2003; Sha & Jackson 2002; Jeloaica & Sidis 1999). This potential is represented in

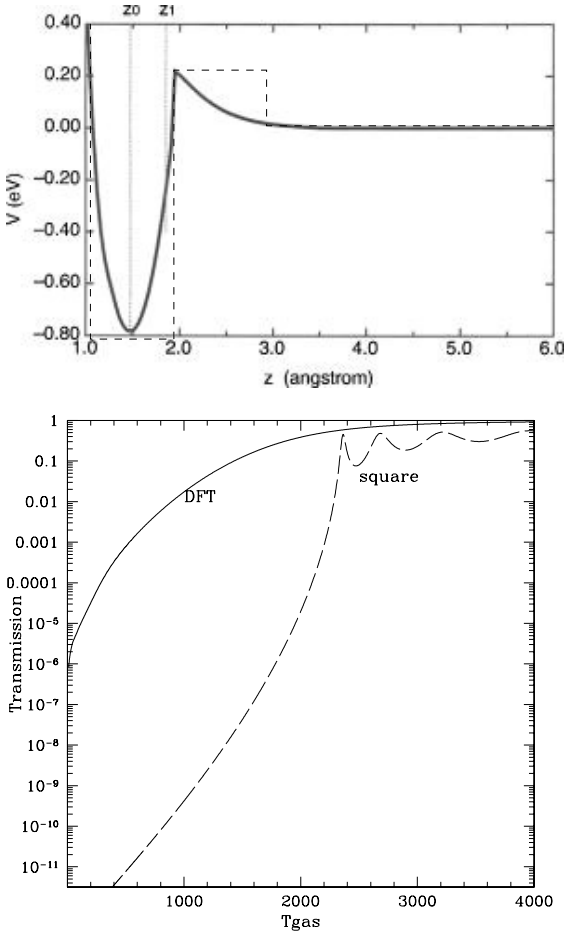

Fig. 1. Transmission coefficients for a square barrier approximation (dotted lines) and for a barrier obtained by DFT calculations (solid lines). *Top panel*: the different barriers considered. *Bottom panel*: transmission coefficients for H and D atoms versus gas temperature.

Fig. 1 as a function of the reaction coordinate z between the H atom and the graphite surface in the collinear approach. The main characteristics of the potential derived from the DFT code PWSCF included in the QUANTUM ESPRESSO package of Giannozzi et al. (2009), are the following:

1. a surface reconstruction is observed: the H can be chemisorbed on the graphite surface on top of a C atom with an energy bond of 0.76 eV. The C atom where H is chemisorbed puckers out of the surface plane;
2. chemisorption on the surface has an associated barrier of 0.2 eV.

The probability of transmission (Fig. 1) of the chemisorption barrier is calculated using the wavepackets propagation method (described in Sect. 2.1) as a function of the incident energy of the H atom coming in from the gas phase. The probability of transmission decreases with decreasing incident energy of the H atom. For energies below 0.2 eV (the value of the chemisorption barrier), the H atom penetrates the barrier by the tunneling effect.

The DFT calculations are performed on a 2×2 working cell. In this case, the chemisorption well is about 0.76 eV and the chemisorption barrier is about 0.2 eV. Casolo et al. (2009) have shown that the chemisorption well is affected by the size of the working cell. For example, for a 5×5 working cell the chemisorption well is 12% higher than with a 2×2 working cell and the chemisorption barrier is 0.15 eV. In our dynamics calculations, we consider a chemisorption barrier 0.2 eV. The value of this barrier will affect the sticking probabilities and the transmission probability of the barrier. For a lower barrier (Casolo et al. 2009) the sticking probabilities and the transmission barrier calculated using dynamics method would be higher than the values calculated here in the energy domain between 0.15 eV and 0.2 eV.

2.3. Sticking of H on graphite using a mixed classical-quantum dynamics method

The detail of the theory to study the sticking of H atom on a graphite surface using the mixed classical-quantum dynamics method is presented in the paper of Morisset et al. (2010). Here, we present a brief description. The Hamiltonian used to describe the interaction of the atom with the dynamical surface is

$$H = T + V_{\rm tot} + H_{\rm b}, \tag{2}$$

where T is the kinetic operator, $V_{\rm tot}$ is the gas-surface potential operator, $H_{\rm b}$ is the Hamiltonian for the lattice vibration without coupling to an atom. In the mixed classical-quantum method, it has the following form:

$$H_{\rm b} = \sum_{i=1}^{N}\sum_{j=1}^{M}\left(\frac{1}{2}w_{ij}\left(Q_{ij}^2 + P_{ij}^2\right)\right), \tag{3}$$

where N and M are the number of phonon modes and phonon bands, respectively. $Q_{\rm ij}$ and $P_{\rm ij}$ are the positions and momenta of the vibrational modes of frequency $w_{\rm ij}$. In the previous papers of Morisset & Allouche (2008, 2010) the Taylor series expansion of the potential $V_{\rm tot}$ in terms of the displacements of the lattice atoms allows one to write the potential as the sum of the static potential $V_0(z)$ between H and the graphite surface in the collinear approach plus an interaction potential between the atom and the bath of phonons. The Taylor expansion is truncated to the linear term in phonon coordinates, which is the one-phonon exchange approximation. In the mixed classical-quantum approach, the total gas-surface interaction can be written as

$$V_{\rm tot} = V_0(z) + \sum_{i=1}^{N}\sum_{j=1}^{M} g_{ij}(z)Q_{ij}, \tag{4}$$

where $g_{ij}(z)$ represents the coupling terms between the motion of H and the bath of phonons with a vibrational mode of frequencies ω_{ij} and a polarization vector ϵ_{ij}. To calculate from DFT calculations the $g_{ij}(z)$ terms, a model has been developed by Morisset & Allouche (2008). The $g_{ij}(z)$ terms are directly calculated of DFT phonon calculation in the harmonic approximation (Ashcroft & Mermin 1976). These calculations allow one to obtain the dynamical matrices D in the irreducible Brillouin Zone (IBZ). By diagonalization of D, the frequencies and polarization vector of the vibrational mode are obtained. The phonon dispersion of the H-graphite system is presented in Fig. 2 of the paper of Morisset & Allouche (2008) along the high-symmetry directions in the IBZ. The phonon dispersion obtained by DFT phonon calculations agree well with previous papers on the subject (Mohr et al. 2007)

The dynamics method is performed through a mixed classical-quantum approach. In this method, the H motion (z coordinate between H and the graphite surface) is treated quantum-mechanically using the wavepackets propagation method (described in Sect. 2.1), whereas each vibrational mode is treated

classically. The time dependence of the classical variables is obtained by solving the equations of motion derived from the Hamilton equations:

$$\dot{Q}_{ij} = \frac{\partial H_{\rm eff}}{\partial P_{ij}},$$
$$\dot{P}_{ij} = -\frac{\partial H_{\rm eff}}{\partial Q_{ij}}, \quad (5)$$

where $H_{\rm eff}$ is the effective Hamiltonian, given by the expectation value of the Hamiltonian H:

$$H_{\rm eff} = < \psi \mid H \mid \psi > . \quad (6)$$

Initially, each vibrational mode obeys the equipartition theorem (McQuarrie 2000): there is $\frac{k_{\rm B}T}{2}$ of energy in each vibrational mode where T is the surface temperature. The wave function is analyzed using the reactive flux as described in Morisset et al. (2010), which allows one to calculate the sticking probability as a function of the incident energy of the H atom and the surface temperature T.

2.4. Dynamics results

2.4.1. Transmission coefficients

In previous studies we calculated the probability for an atom to stick on a grain surface to be equal to the transmission coefficient to cross the barrier against chemisorption (Cazaux & Tielens 2002; Cazaux & Tielens 2004). We considered the barrier to be square and obtained transmission coefficients that strongly depend on the energy of the incoming H atom (see Fig. 1, bottom panel, dotted lines). The transmission coefficients are very small at energies below 0.2 eV (~2320 K, which corresponds to the height of the barrier).

However, the barrier against chemisorption is far from being square. Indeed, DFT calculations show that this barrier varies from 0.79 Å to 1.05 Å in width, with a height of 0.2 eV (see Fig. 1, top panel, Morisset & Allouche 2008). The transmission coefficients obtained with such a barrier are shown as solid lines in Fig. 1, bottom panel. Clearly, the approximation of a square barrier underestimates the transmission coefficients by several orders of magnitude. Already at energies of 1000 K, an H atom would have a 10^7 higher chance to cross a realistic barrier as calculated by DFT than a square barrier. This effect has profound consequences for the sticking of H atoms at low gas temperatures, and will influence which processes govern the formation of H_2 and with what efficiency.

2.4.2. Sticking

In Fig. 2 we present the sticking of H atoms on graphite surfaces calculated with the mixed classical-quantum dynamics method to consider the dissipation of the H atom's energy through the different modes of the lattice. In the present calculation, $N = 11$ phonon bands with $M = 61$ vibrational modes have been included: the phonon bands of C–H (H chemisorbed on the graphite), the four phonon bands of C–C of higher frequencies, the longitudinal mode of C–C, and the three acoustic bands of C–C. Our dynamics calculation shows that the energy exchange between H and the vibrational modes of the substrate takes place by acoustic phonon modes of C–C. The chemisorption barrier (0.2 eV = 2320 K) governs the sticking mechanism: the sticking probability decreases with the incident energy for each surface temperature $T_{\rm dust}$. At incident energies lower than the chemisorption barrier, the sticking coefficient decreases with increasing $T_{\rm dust}$. At low dust temperatures, the surface allows a better dissipation of the energy of the incident atom, and consequently facilitates the sticking. For example, the difference in sticking efficiency on surfaces of 10 K or on surfaces of 125 K can be a factor of 3 for incident energies around 1000 K. At incident energy higher than the chemisorption barrier, the variation of the sticking probability with the surface temperature is negligible.

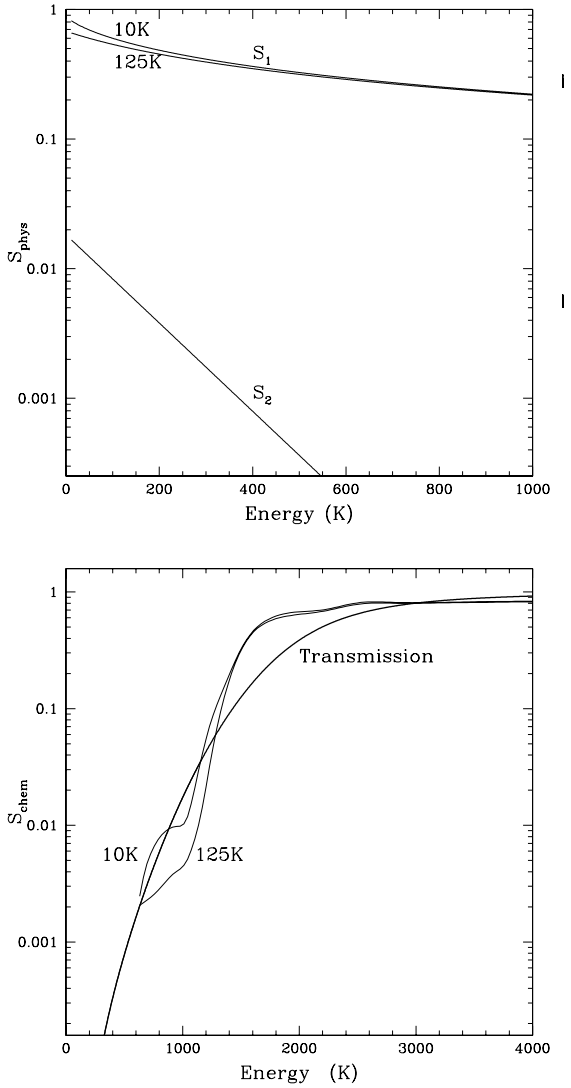

Fig. 2. *Top panel*: sticking probability in physisorbed sites as function of the energy of the incoming H atom according to Cuppen et al. (2010) (S 1, for $T_{\rm dust}$ = 10 and 125 K) and Buch (1989) (S 2). *Bottom panel*: trapping probabilities (transmission) and sticking in chemisorbed sites as function of the energy of the incoming H atom. The transmission coefficient to overcome a barrier derived from DFT calculations is shown as well as the sticking coefficient when the phonons are considered, for $T_{\rm dust}$ = 10 and 125 K.

Our calculation can be compared to experimental work by Zecho et al. (2002). For a surface temperature of 150 K and with a beam centered about 0.2 eV, these authors obtain a sticking probability of 0.5. In our dynamics calculation with the same condition in temperature and energy, the sticking probability is about 0.6. Our results agree well with the experimental work

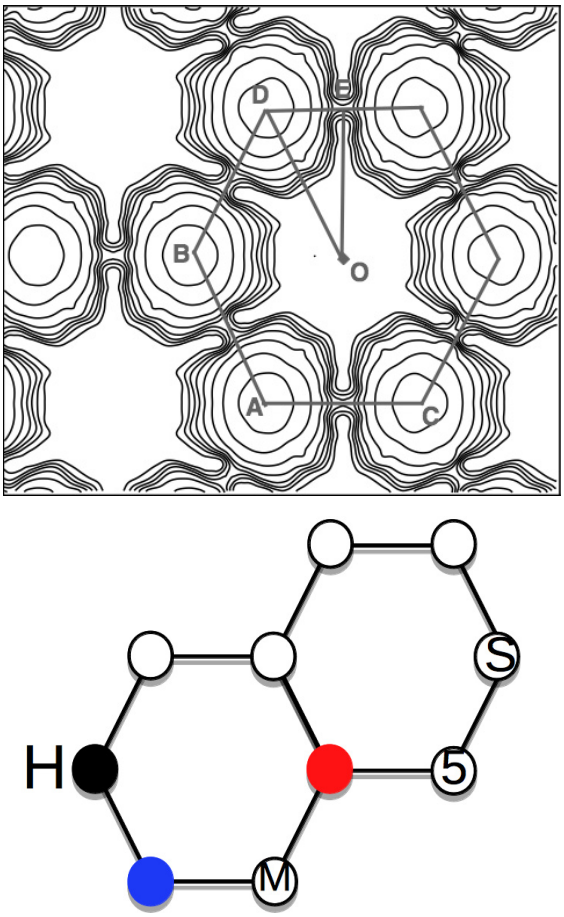

Fig. 3. *Top panel*: contour map of the potential energy surface as a function of the H position on the graphite. The energy difference between two consecutive contour lines is 0.3 eV. A, B, C and D are the positions of a barrier between two chemisorption sites. O is the center of the hexagon. H atoms can chemisorb and physisorb on top of carbon atoms (A, B, C and D), while they can physisorb also in other locations such as a bridge (E). *Bottom panel*: stable configuration for the second H atom: ortho (closer H atom on the hexagon), meta (M) and para (opposite H atom on the hexagon) configurations and 5 and S (second cycle, Dumont et al. 2008)

of Zecho et al. (2002).The other theoretical calculations on the subject have been performed by Sha et al. (2005) and Kerwin et al. (2006), who obtain a probability of 0.1 and 0.0025 in the same domains of energy and temperatures, respectively. These probabilities are smaller because these authors included in their dynamics calculations a coordinate to simulate the energy dissipation in the surface, but do not explicitly take into account the vibrational modes of the substrate. This shows that to study the sticking of an atom on a graphite surface theoretically, it is necessary to take into account the vibrational modes of the surface in the dynamics calculations.

3. H_2 formation using kinetic Monte Carlo simulations

We used a step-by-step Monte Carlo simulation to follow the chemistry occurring on dust grains. This method allows us to follow each individual H atom that arrives, binds and moves on the surface, and formes molecules through different mechanisms. However, this method does not give us informations on the energy of the atoms and formed molecules. The graphite surface is comprised of benzenic rings that allow the H atoms to physisorb or chemisorb, as presented in Fig. 3. H atoms can physisorb above each C atom, and on the bridge between 2 C atoms (position E). However, recent studies showed that H atoms cannot physisorb at the center of the ring (Ferro et al. 2002). The physisorbed energy was chosen to be 43 meV from Ghio et al. (1980) and the barrier between two physisorbed sites is almost negligible (5–7 meV, Bonfanti et al. 2007). H atoms can chemisorb on top of C atoms with an associated barrier of 0.2 eV and an energy of 0.76 eV. If an atom is already present on a ring, a second atom, with a spin opposite to the adsorbed atom, can become chemisorbed in a para configuration without a barrier (Rougeau et al. 2006), making a para-dimer. H atoms can also become chemisorbed in ortho and meta configurations, but these processes are associated with a barrier of 0.26 and 0.16 eV, respectively (Rougeau et al. 2006). The para-dimer is the favored configuration to form H_2 because it is barrier-less compared to the other configuration. A third atom arriving on this dimer can create an H_2 molecule without a barrier (Bachellerie et al. 2007). If an atom from the gas phase arrives on an adsorbed atom (a monomer), then there is a barrier of 9 meV, as derived by Morisset et al. (2004a).

Species that are accreted from the gas phase arrive at a random time and location on the dust surface. This arrival time depends on the rate at which gas species collide with the grain. This accretion rate can be written as:

$$R_{\rm acc} = n_{\rm H} v_{\rm H} \sigma S, \tag{7}$$

where $n_{\rm H}$ and $v_{\rm H}$ are the density and velocity of the H atoms in the gas, σ is the cross section of the dust particle and S is the sticking coefficient of the H atoms with the dust. The sticking in chemisorbed sites has been discussed above. This coefficient strongly depends on the form of the barrier to chemisorb, but is also somewhat sensitive to the surface temperature because energy transfer to or from the phonon can be important to loose excess energy. In Fig. 2, top panel, different sticking probabilities for the physisorption case are presented as a function of gas temperature ($T_{\rm gas}$). In this figure, $S1$ represents the sticking probability derived by Cuppen et al. (2010) based on a soft cube model:

$$S_{\rm phys} = (1 + a_1 \sqrt{T_{\rm gas} + T_{\rm grain}} + a_2 T_{\rm gas} - a_3 T_{\rm gas}^2)^{-1}, \tag{8}$$

with $a_1 = 4.2 \times 10^{-2}$ K$^{-1/2}$, $a_2 = 2.3 \times 10^{-3}$ K^{-1}, and $a_3 = 1.3 \times 10^{-7}$ K^{-2}. $S1$ decreases with the energy of the gas. At 100 K, $S1 = 0.8$ while it becomes 0.2 at 1000 K. At low $T_{\rm gas}$, $S1$ is sensitive to the temperature of the dust. The sticking probability of H in physisorbed sites on graphite is important in this model. $S2$ represents the sticking probability obtained by Buch (1989). This model is based on the quantum mechanical perturbation theory. This calculation includes a microscopic description of the solid structure and vibrations. $S2$ is very weak and varies between 0.02 and 10^{-4} in the energy domain $T_{\rm gas} = 50$–550 K.

Atoms arriving from the gas phase on top of a carbon atom can either be physisorbed (with a sticking efficiency $S_{\rm phys}$) or be chemisorbed (with a sticking efficiency $S_{\rm chem}$). In our model, H atoms mostly arrive from the gas phase in physisorbed sites for low temperature gas, because of the high barrier to access chemisorbed sites.

The species that are present on the surface can go back into the gas phase through evaporation. The evaporation rate of

H atoms in physisorbed or chemisorbed sites can be written as

$$R_{\mathrm{evap}(H_p)} = \nu_p \times \exp\left(-\frac{E_p}{k_B T}\right), \quad (9)$$
$$R_{\mathrm{evap}(H_c)} = \nu_c \times \exp\left(-\frac{E_c}{k_B T}\right),$$

where E_p and E_c are the binding energies of the H atom in a physisorbed or chemisorbed site, respectively, and ν_p and ν_p are the oscillation factors of the atoms in the physisorbed and chemisorbed sites taken as $\nu_p = 10^{12}$ s^{-1} and $\nu_c = 10^{13}$ s^{-1}.

The species that arrive at a location on the surface can move randomly through tunneling effects and thermal hopping. The diffusion rates for an atom to go from one physisorbed to another physisorbed site (R_{pp}), and for an atom to go from a physisorbed site to a chemisorbed site (R_{pc}) can be written as:

$$R_{pp} = \nu_p \times \exp(-\frac{E_{pp}}{k_B T}),$$
$$R_{pc} = \nu_p \times P_{pc}, \quad (10)$$

where P_{pc} is the probability for the atom to go from a physisorbed site to a chemisorbed site by tunneling effects or thermal hopping, as described in Cazaux & Tielens (2004). When thermal hopping dominates, which is usually the case for high temperatures or when the barrier is low, this probability can be written as $P_{pc} = \exp(-\frac{E_{pc}}{k_B T})$, where E_{pc} is the energy of the barrier between the physisorbed and the chemisorbed site. This barrier is 0.2 eV, which means that physisorbed H atoms cannot directly reach chemisorbed sites. However, if a chemisorbed atom is already present, then the barrier in its associated para-site disappears. In this case, the physisorbed H atom can reach these para-sites without a barrier and consequently will hop thermally in chemisorption.

The mechanisms included in our KMC simulations are the mechanisms M1 to M5 described in the introduction. Dumont et al. (2008) have included the formation of ortho, para, meta, and 5 and S dimers (see Fig. 3, bottom panel) in their KMC calculations . The H atoms can diffuse from one dimer position to another. These simulations explained the occurrence of two peaks in the thermal recombinative desorption of molecular H_2 from clean graphite surfaces, after chemisorption of H atoms. The first peak (450 K) is essentially caused by the para-dimer desorption, whereas the second peak (560 K) is caused by the ortho-dimer desorption. The other mechanisms included in their simulation contribute to the H_2 desorption, but with a small amount. In this work we concentrate on H_2 formation on dust grains with temperatures below 150 K. The mechanisms considered by Dumont et al. (2008) are not relevant for the range of temperatures considered in this study because diffusion of chemisorbed H atoms as well as thermal recombinative desorption occur at much higher temperatures. In this study we use similar mechanisms as were considered in Cuppen & Hornekær (2008), and also include the formation of H_2 with two physisorbed atoms.

The mechanisms to form H_2 are associated with very high barriers if they involve a chemisorbed H atom in a monomer (mechanisms 2 and 4), and are barrier-less if chemisorbed H atoms in para-dimers are involved. We performed several simulations for the formation of H_2 on graphitic surfaces with various grain and gas temperatures. We first considered the barrier to enter chemisorbed sites as being square, and then considered more realistic barriers obtained by DFT calculations. Finally, we also took into account the effect of the phonons on the sticking of atoms in chemisorbed sites.

In our simulations we calculated the total sticking coefficient times the total H_2 efficiency, $S \times \epsilon$. This product can be written

$$S \times \epsilon = S_{\mathrm{phys}} \times \epsilon_{\mathrm{phys}} + S_{\mathrm{chem}} \times \epsilon_{\mathrm{chem}}, \quad (11)$$

where $S_{\mathrm{phys}} \times \epsilon_{\mathrm{phys}}$ is the product of the sticking coefficient in physisorbed sites times the H_2 efficiency involving physisorbed atoms, and $S_{\mathrm{chem}} \times \epsilon_{\mathrm{chem}}$ is the product of the sticking coefficient in chemisorbed sites times the H_2 efficiency involving chemisorbed atoms. The efficiency of H_2 formation is written as

$$\epsilon = \frac{2 \times n_{H_2}}{n_H}, \quad (12)$$

where n_{H_2} is the number of H_2 molecules formed, and n_H the number of H atoms that arrived on the surface.

3.1. Effect of the barrier on H_2 formation

The transmission probability for H atoms to overcome the chemisorption barrier (0.2 eV) in the collinear approach is calculated following two different approximations:

1) the chemisorption barrier is considered as a square barrier (Fig. 1, bottom panel, dashed lines). The transmission probability is presented in Fig. 1, top panel (dashed lines);
2) the chemisorption barrier is obtained by DFT calculations (Fig. 1, bottom panel, solid lines) using the wavepacket propagation method described in Sects. 2.1 and 2.2, and the transmission probability is presented in Fig. 1, top panel (solid lines).

The simulations for the formation of H_2 considering a square barrier and a barrier obtained by DFT calculations to enter chemisorbed sites are shown in Figs. 4 and 5. The square barrier model has been used in previous studies (Cazaux & Tielens 2002, 2004). The objective of this study is to understand the influence of the form of the chemisorption barrier on the H_2 formation using the KMC simulations. For the H_2 formation, mechanisms M1 to M5 are included in the KMC simulations. In Fig. 4 and 5 ϵ_1 represents the efficiency of H_2 formation when a square barrier is considered, while ϵ_2 represents the same efficiency when the barrier is obtained by DFT calculations. We considered temperatures of the gas of 100, 500, 1000 and 2000 K with grain temperatures from 8 to 90 K. Our results show that at low dust temperatures ($T_{\mathrm{dust}} < 15$ K for barrier 1 and <20 K for barrier 2), the formation of H_2 involves physisorbed atoms, either with the mechanism M1 (2 physisorbed atoms) or with the mechanism M5 (one physisorbed atom entering a chemisorbed site occupied by an H atom in a dimer). The efficiency to form H_2 at these temperatures is on the order of 100%, and therefore the product $S \times \epsilon$ is equal to S_{phys}. At dust temperatures higher than ~15 K, the physisorbed atoms evaporate, and molecular hydrogen is formed with chemisorbed atoms. The type of barrier considered has a very significant effect on the formation of H_2 because it determines the sticking of H atoms in chemisorbed sites. At low gas temperatures the H atoms have a low probability to enter the chemisorbed sites, and therefore the formation efficiency is low. H_2 is formed through the direct Eley-Rideal mechanism when an H atom from the gas arrives on a dimer on the surface (M3). Once a first H atom sticks to one chemisorbed site, the second one sticks to a para-site without a barrier, and a third H atom coming on the dimer can form an H_2 molecule

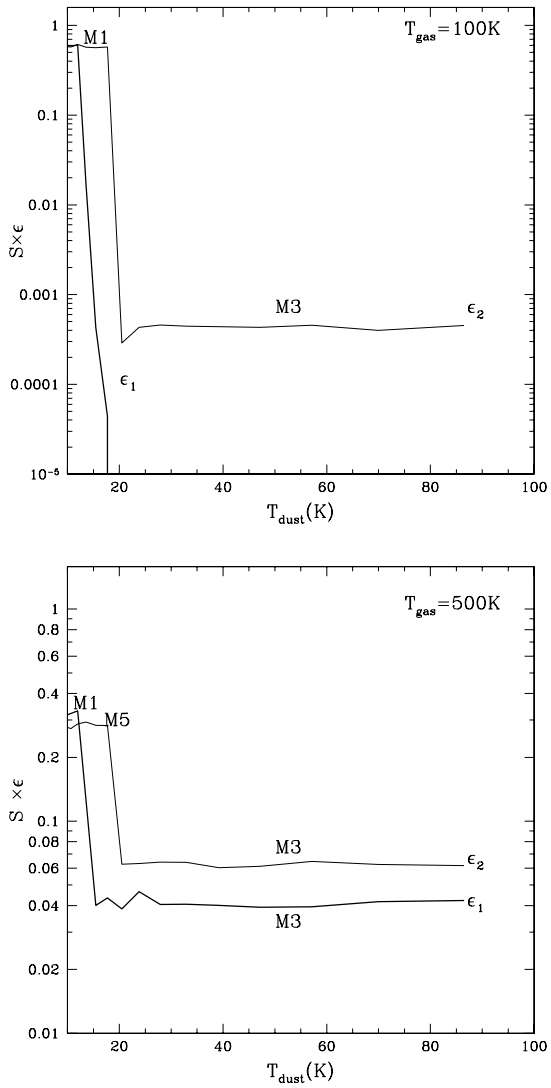

Fig. 4. H_2 formation efficiencies when squared barriers (ϵ_1) and DFT barriers (ϵ_2) are considered to enter in chemisorbed sites. The mechanisms important for the formation of H_2 are M1 (2 physisorbed atoms), M2 (direct chemisorption with H monomer), M3 (direct chemisorption with H dimer) and M5 (physisorbed atom entering chemisorbed sites with H dimer) .

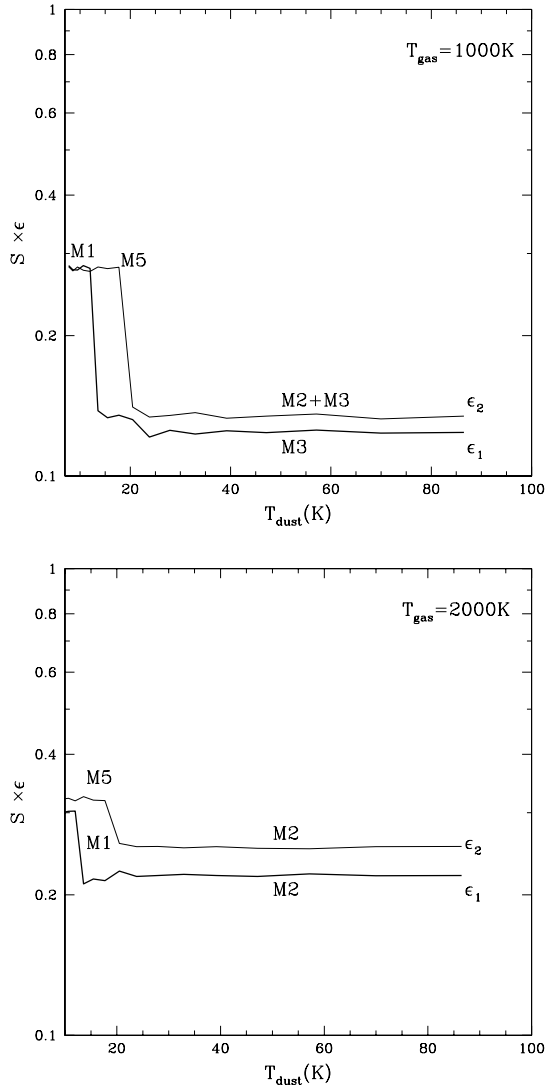

Fig. 5. Same as Fig. 4 for $T_{\rm gas}$ = 1000 and 2000 K.

without a barrier. The atom that stays on the surface is used to make another dimer, again without a barrier, and another H_2 molecule can be formed. With this process, $S \times \epsilon$ is several orders of magnitude higher than the sticking alone. As the gas temperature increases, the barrier to become chemisorbed becomes easier to overcome, and H_2 can form through the direct Eley-Rideal mechanism when an H atom from the gas arrives on a single H on the surface (M2).

3.2. Effects of the surface dynamics on the formation of H_2

We used KMC simulations including mechanisms M1 to M5 to calculate the formation of H_2 on dust surfaces of 10 and 125 K as function of the gas temperature. The atoms present in the gas phase arrive on the surface with an energy that allows them either to stick in chemisorbed sites (if the barrier to chemisorption can be overcome), or to stick in physisorbed sites (if atoms can thermalize in physisorbed sites), or to bounce back to the gas phase. For the two surface temperatures considered, the sticking in chemisorption was calculated above (Sect. 2.4.2), taking into account the effect of surface dynamics. However, the sticking in physisorption varies strongly from one study to another. In this work we consider strong sticking in physisorption (Cuppen et al. 2010), and weak sticking in physisorption (Buch 1989), and calculate the product of sticking times efficiency for H_2 formation, $S \times \epsilon$, for each case.

3.2.1. Strong sticking in physisorption

In Fig. 6 (top panel) we show the product $S \times \epsilon$ for surface temperatures of 10 and 125 K, and for gas temperatures varying from 100 to 3000 K. This product is the sum of the H_2 formation efficiency times sticking involving physisorbed atoms, $S_{\rm phys} \times \epsilon_{\rm phys}$, and involving chemisorbed atoms, $S_{\rm chem} \times \epsilon_{\rm chem}$. In these calculations, we consider a sticking coefficient for physisorption, $S_{\rm phys}$, such as the one in Cuppen et al. (2010), and shown in Fig. 2. For $T_{\rm dust}$ = 10 K, $S \times \epsilon$ is very large at low gas temperatures and decreases as gas temperature increases. Because of the high sticking probability to physisorb, the formation of H_2 involves physisorbed atoms and therefore $S \times \epsilon$

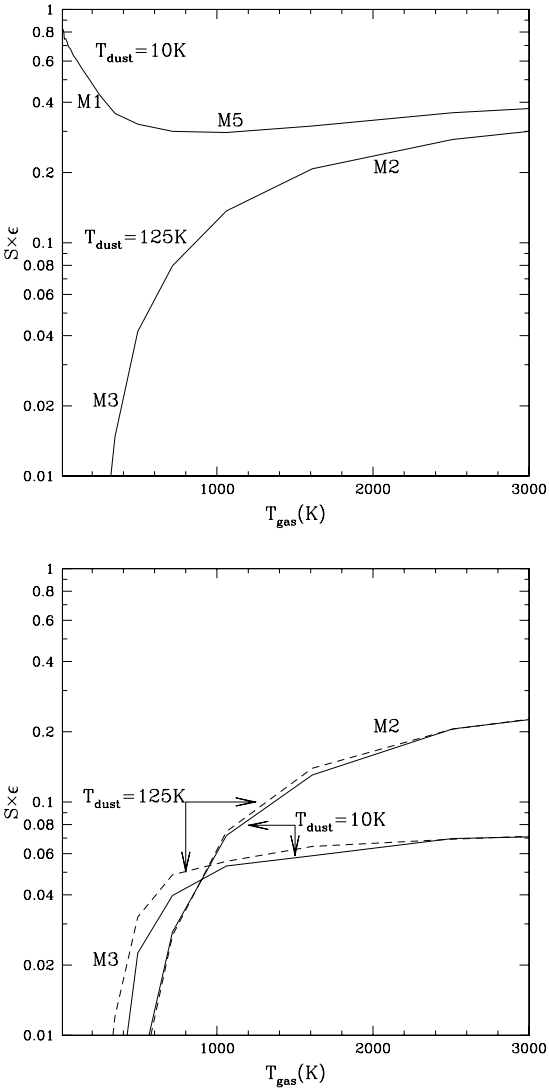

Fig. 6. H_2 formation efficiencies on 10 K and 125 K surfaces as a function of gas temperature, with the sticking in physisorbed sites S_{phys} taken as in Cuppen et al. (2010). *Top*: total H_2 formation, governed by mechanisms M1 (2 physisorbed atoms) and M5 (physisorbed atom arriving in H dimer) for 10 K dust, and governed by mechanisms M3 (direct chemisorption with H dimer) and M2 (direct chemisorption with H monomer). *Bottom*: same as top panel but for H_2 formation involving only chemisorbed atoms. At low gas temperatures, H_2 is formed through mechanism M3 (direct chemisorption with H dimer). For $T_{gas} > 1000$ K, H_2 is formed though mechamism M2 (direct chemisorption with H monomer).

depends on S_{phys}. At gas temperatures lower than 500 K, H_2 is formed through the association of two physisorbed atoms (mechanism M1), while for higher gas temperatures, physisorbed atoms enter chemisorbed sites and associate with H atoms in a dimer (mechanism M5). For $T_{dust} = 125$ K, $S \times \epsilon$ is very small at low gas temperatures and increases as the gas temperature increases. Because of the high surface temperature, physisorbed atoms do not stay on the surface and the formation of H_2 is ensured by chemisorbed atoms. The formation of H_2 proceeds through direct Eley-Rideal mechanisms involving a chemisorbed H atom in a dimer (M3), for $T_{gas} < 1000$ K, and involving an chemisorbed H atom in a monomer for higher T_{gas} (M2). For the two different surface temperatures considered, the

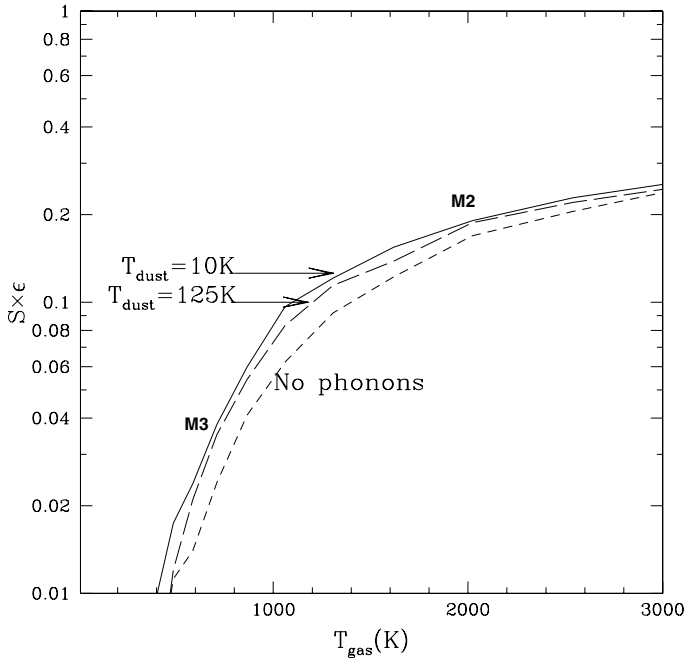

Fig. 7. Same as Fig. 6 with the sticking in physisorbed sites S_{phys} taken as in Buch (1989).

mechanisms to form H_2 are different because they either involve physisorbed atoms (for $T_{dust} = 10$ K) or chemisorbed atoms (for $T_{dust} = 125$ K). However, the effects of surface dynamics on the formation of H_2 can be appreciated only by comparing the formation of H_2 involving chemisorbed atoms. For this purpose we represent in Fig. 6 (bottom panel) the different contributions for the formation of H_2 that involve only chemisorbed atoms; $S_{chem} \times \epsilon_{chem}$. The different mechanisms for the formation of H_2 that involve only chemisorbed atoms are shown as dashed lines for $T_{dust} = 125$ K and solid lines for $T_{dust} = 10$ K. For $T_{gas} < 1000$ K, H_2 forms through Eley-Rideal mechanisms involving a chemisorbed H atom in a dimer (M3), while for higher T_{gas}, H atoms can access chemisorbed sites easily even with a barrier, and H_2 is ensured through Eley-Rideal mechanisms involving a chemisorbed H atom in a monomer (M2). The product $S_{chem} \times \epsilon_{chem}$ slightly depends on the surface temperature, but the effect of the surface dynamics cannot be assessed. Indeed, the mechanism involving chemisorption depends also on the physisorption because many physisorbed atoms can travel on the surface and become chemisorbed. Therefore, as long as some H atoms can become physisorbed and subsequently reach the chemisorbed sites, it is not possible to really isolate the impact of surface dynamics on the formation of H_2.

3.2.2. Weak sticking in physisorption

In Fig. 7 we present the same calculations as previously, but we now consider a very small sticking coefficient for physisorption, S_{phys}, as described in Buch (1989). In this case, $S_{phys} = 0.02$ at low gas temperatures and S_{phys} decreases exponentially as T_{gas} increases (see Fig. 2). Our results show that because atoms do not stick in physisorbed sites, H_2 formation is ensured by mechanisms involving only chemisorbed atoms. For $T_{gas} < 1000$ K, H_2 forms through Eley-Rideal mechanisms involving a chemisorbed H atom in a dimer (M3), while for higher T_{gas}, gas phase H atoms can enter chemisorbed sites even if there

is a barrier, and H_2 formation is ensured through Eley-Rideal mechanisms involving a chemisorbed H atom in a monomer (M2). The total product $S \times \epsilon$ is equal to $S_{\rm chem} \times \epsilon_{\rm chem}$, and the effects of the surface dynamics on the sticking in chemisorption can be addressed. If the surface is flat (represented as small dashed lines), then $S_{\rm chem}$ is smaller (see Fig. 2) and the product is therefore smaller. When the surface dynamics are considered, the sticking $S_{\rm chem}$ is more efficient, and therefore the product $S \times \epsilon$ is slightly higher. We also note that the effect of the surface temperature on the product $S \times \epsilon$ is almost negligible, as shown by the curves for $T_{\rm dust} = 10$ K (solid) and $T_{\rm dust} = 125$ K (small dashed).

4. Discussion and conclusions

We have studied the influence of the sticking probability on the formation of H_2 using KMC simulations. In our model, mechanisms M1 to M5 (described in the introduction) for the H_2 formation are included. We have determined the predominant mechanisms to form H_2 as function of gas and dust temperatures.

First, we assumed the sticking probability of H atoms to be equal to the transmission coefficient to cross the barrier against chemisorption. To address the significance of the shape of the barrier, we considered a square barrier and a barrier obtained by DFT calculations. For the latter, wavepacket propagation calculations along the coordinate between the H atom and the graphite surface (collinear approach) were performed to determine the transmission probabilities of the chemisorption barrier. Our results show that if a square barrier is considered, the transmission probabilities are underestimated by many orders of magnitude at low gas temperatures ($T_{\rm gas} \leq 2000$ K). The impact of the form of the barrier is visible in the results of the KMC calculations simulating the formation of H_2. Our results show that the shape of the chemisorption barrier (square or obtained by DFT) has a strong impact on the H_2 formation for $T_{\rm dust} \geq 15$ K. This impact increases as gas temperatures decrease. In conclusion, the formation of H_2 calculated with barriers obtained by DFT is much more efficient than with square barriers. In these temperature domains, H_2 formation involves chemisorbed atoms. For $T_{\rm dust} \leq 15$ K, H_2 is formed by a physisorption mechanism. In this case, the form of the chemisorption barrier is not important.

Second, we investigated the sticking of H atoms in chemisorbed sites taking into account the vibrational modes of the surface. For this we used a mixed classical-quantum dynamics method where the motion of the H atom is treated quantum-mechanically, while the vibrational modes of the surface are treated classically (Morisset & Allouche 2008). The sticking probability, which takes into account the vibrational modes of the surface, can be compared to the transmission probability of the barrier. The sticking probability is higher by a factor of 5 for $T_{\rm gas} \sim 1500$ K, but is lower by a factor 2 (for $T_{\rm dust} = 10$ K) to 5 (for $T_{\rm dust} = 125$ K) around $T_{\rm gas} \sim 1000$ K. This calculation shows that the energy exchange between the atom and the bath of phonon is higher than the transmission probability of the chemisorption barrier. These sticking probabilities are calculated as a function of $T_{\rm gas}$, for $T_{\rm dust} = 10$ K and $T_{\rm dust} = 125$ K. We implemented these sticking coefficients $S_{\rm chem}$ in our KMC simulations and showed that for $T_{\rm dust} = 125$ K, H_2 is formed through a chemisorption mechanism (involving dimers for $T_{\rm gas} \leq 1000$ K and monomers for $T_{\rm gas} \geq 1000$ K). For $T_{\rm dust} = 10$ K, on the other hand, H_2 formation involves physisorbed atoms if the sticking in physisorption is high. In this case the efficiency to form H_2 depends of the sticking probabilities of H atom in a physisorption site.

The sticking in physisorption influences the formation of H_2 at low dust temperatures (≤15 K). In this study we considered two possible sticking coefficients in physisorption $S_{\rm phys}$. 1) The sticking derived in Cuppen et al. (2010), which is valid for metals and is close to unity for low gas and dust temperatures. 2) The sticking derived by Buch (1989), which shows that the probability of sticking for H atoms on graphite is on the order of a few percent (Lepetit et al. 2011; Medina & Jackson 2008). The influence of this $S_{\rm phys}$ on the product $S \times \epsilon$ is very significant at low dust temperatures. If the sticking is taken as in 1), then H_2 is formed through LH mechanisms with physisorbed atoms, and $S \times \epsilon$ is very high $\sim S_{\rm phys}$. On the other hand, if the sticking in physisorption is chosen to be as in 2), the formation of H_2 involving physisorbed atoms is not efficient, and the formation of H_2 is ensured by chemisorbed H atoms. In this case, the product $S \times \epsilon$ depends on $S_{\rm chem} \times \epsilon_{\rm chem}$. Our KMC simulations show that once the vibrational modes of the H-graphite system are taken into account in the sticking, the efficiency to form H_2 is increased by a factor 2. This behavior is not surprising because the sticking probability obtained by dynamics calculations is higher than the value of the transmission probability of the chemisorption barrier.

In the ISM the H_2 molecules formed are ro-vibrationally excited. The excitation of the molecule is caused by the energy transfer of the kinetic energy toward the substrate, the translational energy and the excitation of the molecule. The ro-vibrational excitation of the molecule allows the determination of the mechanisms to form H_2 (Lemaire et al. 2010; Islam et al. 2007). Different mechanisms have been studied theoretically by several groups (Rutigliano et al. 2001; Ree et al. 2002; Sha & Jackson 2002; Morisset et al. 2003; Morisset et al. 2004a; Morisset et al. 2005; Martinazzo & Tantardini 2006; Bachellerie et al. 2007). In our KMC simulations it is not possible to extract the energy of the H_2 formed. These simulations only allow us to follow the number of molecules formed through different mechanisms (M1 to M5 described in the introduction). We determined the predominant mechanism to form H_2 as a function of the dust and gas temperatures.

Recently, Cuppen et al. (2010) performed similar work on the formation of H_2 and the influence of the sticking on the product $S \times \epsilon$. These authors concentrated on the sticking in physisorbed sites (and we used their results in this work), but assumed that the atoms from the gas phase had to thermally overcome the barrier against chemisorption to become chemisorbed. In this sense, the H atoms coming from the gas phase do not stick in chemisorbed sites at low $T_{\rm gas}$ ($S_{\rm chem} = 0.03$, 0.0001 and 10^{-8} for $T_{\rm gas} = 500$, 200 and 100 K, respectively). Therefore, our results are similar to Cuppen et al. (2010) for cold dust, when physisorbed atoms are involved to form H_2. However, on warm dust grains (~100 K), chemisorbed atoms are needed to form H_2 and the sticking of H atoms in chemisorbed sites sets the formation of H_2. In this case, our results diverge from Cuppen et al. (2010) for gas temperatures lower than 500 K, because we consider that H atoms from the gas phase can tunnel through the important barrier against chemisorption. This process makes the sticking of H atoms in chemisorbed sites still efficient at low $T_{\rm gas}$. Once these chemisorbed sites are populated, H_2 can form efficiently through barrier-less routes involving the creation of dimers. Therefore, our results show that the formation of H_2 is efficient for intermediate gas and dust temperatures as well ($T_{\rm dust} > 15$ K and 1000 K > $T_{\rm gas} > 100$ K).

Our results suggest that the formation of H_2 remains efficient in regions where gas and dust are warm. This is true if the time for H atoms to enter chemisorbed sites is shorter than other routes to form H_2 (i.e. dense and warm medium). Therefore, the grain surface route proposed in this study should be compared to other routes to form H_2. Environments where grain surface chemistry would dominate to form H_2 include photon dominated regions (PDRs, Hollenbach & Tielens 1999), X-ray dominated regions (XDRs, Meijerink & Spaans 2005), hot cores (Caselli et al. 1993), and the early universe (Cazaux & Spaans 2004, 2009). Particularly PDRs and XDRs enjoy regions of upto 10^{22} and 10^{24} cm^{-2}, respectively, where rapid photo-dissociation and chemical removal of H_2 requires it to be formed efficiently on dust grains to drive ion-molecule chemistry and H_2 line emission (Habart et al. 2004). In PDRs and XDRs gas temperatures can be as high as 10^3 K (Meijerink et al. 2007), values for which the traditional sticking coefficient of Hollenbach & McKee (1979) decreases rapidly. At early cosmic epochs, for redshifts higher than 10, the first grain surfaces are expected to be warm, at least 30 K, due to the strong cosmic microwave background. Furthermore, the low abundances of metals like carbon and oxygen cause gas temperatures to be 10^2–$10^{3.5}$ K and to be set mostly by H_2 and HD cooling (Glover & Abel 2008). Our results indicate that chemisorption effects allow dust grains to act as catalysts for H_2 formation under such hostile primordial conditions.

Acknowledgements. The authors wish to thank the anonymous referee for her/his constructive comments. S.C. is supported by the Netherlands Organization for Scientific Research (NWO). The authors wish to thank CINES for allowing them to use its computational facilities. This work is supported by the Euratom-CEA Association, in the framework of the Fédération de Recherche Fusion par Confinement Magnétique, and by the Agence Nationale de la Recherche (ANR CAMITER ANR-06-BLAN-0008-01).

References

Ashcroft, N. W., & Mermin, N. 1976, Solid State Physics. (New York: Holt, Rinehart and Winston)
Bachellerie, D., Sizun, M., Teillet-Billy, D., Rougeau, N., & Sidis, V. 2007, Chem. Phys. Lett., 448, 223
Balint Kurti, G., Dixon, R., & Martson, C. 1990, J. Chem. Soc. Faraday Trans., 86, 1741
Bonfanti, M., Martinazzo, R., Tantardini, G. F., & Ponti, A. 2007, J. Phys. Chem. C, 111, 5825
Buch, V. 1989, J. Chem. Phys., 91, 4974
Burke, J. R., & Hollenbach, D. J. 1983, ApJ, 265, 223
Caselli, P., Hasegawa, T. I., & Herbst, E. 1993, ApJ, 408, 548
Casolo, S., Lø vvik, O. M., Martinazzo, R., & Tantardini, G. F. 2009, J. Chem. Phys., 130
Cazaux, S., & Spaans, M. 2004, ApJ, 611, 40
Cazaux, S., & Spaans, M. 2009, A&A, 496, 365
Cazaux, S., & Tielens, A. G. G. M. 2002, ApJ, 575, L29
Cazaux, S., & Tielens, A. G. G. M. 2004, ApJ, 604, 222
Cuppen, H. M., & Hornekær, L. 2008, J. Chem. Phys., 128, 174707
Cuppen, H. M., Kristensen, L. E., & Gavardi, E. 2010, MNRAS, 406, L11
Dumont, F., Picaud, F., Ramseyer, C., et al. 2008, Phys. Rev. B, 77, 223401
Ferro, Y., Marinelli, F., & Allouche, A. 2002, J. Chem. Phys., 116, 8124
Ferro, Y., Marinelli, F., & Allouche, A. 2003, Chem. Phys. Lett., 368, 609
Ferro, Y., Teillet-Billy, D., Rougeau, N., et al. 2008, Phys. Rev. B, 78, 085417
Ghio, E., Mattera, L., Salvo, C., Tommasini, F., & Valbusa, U. 1980, J. Chem. Phys., 73, 556
Giannozzi, P., Baroni, S., Bonini, N., et al. 2009, J. Phys. Cond. Matt., 21, 5502
Glover, S. C. O., & Abel, T. 2008, MNRAS, 388, 1627
Gould, R. J., & Salpeter, E. E. 1963, ApJ, 138, 393
Habart, E., Boulanger, F., Verstraete, L., Walmsley, C. M., & Pineau des Forêts, G. 2004, A&A, 414, 531
Hollenbach, D., & McKee, C. F. 1979, ApJS, 41, 555
Hollenbach, D. J., & Tielens, A. G. G. M. 1999, Rev. Mod. Phys., 71, 173
Hornekær, L., Rauls, E., Xu, W., et al. 2006, Phys. Rev. Lett., 97, 186102
Islam, F., Latimer, E. R., & Price, S. D. 2007, J. Chem. Phys., 127, 064701
Jeloaica, L., & Sidis, V. 1999, Chem. Phys. Lett., 300, 157
Kerwin, J., Sha, X., & Jackson, B. 2006, J. Phys. Chem. B, 110, 18811
Kosloff, D., & Kosloff, R. 1983, J. Comput. Phys., 52, 35
Leforestier, C., Bisseling, R. H., Cerjan, C., et al. 1991, J. Comput. Phys., 94, 59
Leitch-Devlin, M. A., & Williams, D. A. 1985, MNRAS, 213, 295
Lemaire, J. L., Vidali, G., Baouche, S., et al. 2010, ApJ, 725, L156
Lepetit, B., Lemoine, D., Medina, Z., & Jackson, B. 2011, J. Chem. Phys., 134, 114705
Martinazzo, R., & Tantardini, G. F. 2006, J. Chem. Phys., 124, 124703
McQuarrie, D. A. 2000, Stat. Mech. (Sausalito, CA: University Science Books)
Medina, Z., & Jackson, B. 2008, J. Chem. Phys., 128, 114704
Meijerink, R., & Spaans, M. 2005, A&A, 436, 397
Meijerink, R., Spaans, M., & Israel, F. P. 2007, A&A, 461, 793
Mennella, V. 2006, ApJ, 647, L49
Mohr, M., Maultzsch, J., Dobardžić, E., et al. 2007, Phys. Rev. B, 76, 035439
Morisset, S., & Allouche, A. 2008, J. Chem. Phys., 129, 024509
Morisset, S., Aguillon, F., Sizun, M., & Sidis, V. 2003, Chem. Phys. Lett., 378, 615
Morisset, S., Aguillon, F., Sizun, M., & Sidis, V. 2004a, J. Chem. Phys., 121, 6493
Morisset, S., Aguillon, F., Sizun, M., & Sidis, V. 2004b, J. Phys. Chem. A, 108, 8571
Morisset, S., Aguillon, F., Sizun, M., & Sidis, V. 2005, J. Chem. Phys., 122, 1
Morisset, S., Ferro, Y., & Allouche, A. 2010, J. Chem. Phys., 133, 044508
Perry, J. S. A., & Price, S. D. 2003, Ap&SS, 285, 769
Pirronello, V., Biham, O., Liu, C., Shen, L., & Vidali, G. 1997a, ApJ, 483, L131
Pirronello, V., Liu, C., Shen, L., & Vidali, G. 1997b, ApJ, 475, L69
Pirronello, V., Liu, C., Roser, J. E., & Vidali, G. 1999, A&A, 344, 681
Pirronello, V., Biham, O., Manicó, G., Roser, J. E., & Vidali, G. 2000, in Molecular Hydrogen in Space, ed. F. Combes, & G. Pineau Des Forets, 71
Ree, J., Kim, Y., & Shin, H. 2002, Chem. Phys. Lett., 353, 368
Rougeau, N., Teillet-Billy, D., & Sidis, V. 2006, Chem. Phys. Lett., 431, 135
Rutigliano, M., Cacciatore, M., & Billing, G. 2001, Chem. Phys. Lett., 340, 13
Sha, X., & Jackson, B. 2002, Surface Science, 496, 318
Sha, X., Jackson, B., Lemoine, D., & Lepetit, B. 2005, J. Chem. Phys., 122, 014709
Spaans, M., & Silk, J. 2000, ApJ, 538, 115
Weingartner, J. C., & Draine, B. T. 2001, ApJ, 548, 296
Zecho, T., Guttler, A., Sha, X., Jackson, B., & Kuppers, J. 2002, J. Chem. Phys., 117, 8486